Electronic Supplementary Material (ESI) for RSC Advances.

Supporting information for:

Nanoporous Nitrogen Doped Graphene: An Efficient Metal-free Electrocatalyst for Oxygen Reduction Reaction

Amir Yadegari [1,2], Leila Samiee [3], Saeedeh Tasharrofi [3], Sanaz Tajik [4], Alimorad Rashidi [3],
Fatemeh Shoghi [5], Morteza Rasoulian Boroujeni [2], Mohammadreza Tahriri [2], Samuel J.
Rowley-Neale,[6,7] and Craig E. Banks[6,7]

[1] *School of Chemical Engineering, College of Engineering, University of Tehran, P.O. Box: 11155-4563, Tehran, Iran*

[2] *Department of Developmental Sciences, Marquette University, Milwaukee, WI 53233, USA*

[3] *Research Institute of Petroleum Industry (RIPI), West Entrance Blvd., Olympic Village, P.O. Box: 14857-33111, Tehran, Iran*

[4] *Faculty of Chemical Engineering, Amirkabir University of Technology, Hafez Ave, P.O. Box 15875-4413, Tehran, Iran*

[5] *Department of Chemistry, Université de Montréal, 2900 Boulevard Edouard-Montpetit, Montréal, QC H3T 1J4, Canada*

[6] *Faculty of Science and Engineering, Manchester Metropolitan University, Manchester, M1 5GD, UK*

[7] *Manchester Fuel Cell Innovation Centre, Manchester Metropolitan University, Chester Street, Manchester M1 5GD, UK.*

XPS was performed to investigate the elemental composition of the electrocatalysts and verify the degree and type of nitrogen doping. As clearly seen in Supporting information, Figure S2a, the XPS survey of porous graphene shows two distinctive peaks at 285 and 531eV corresponding to C1s and O1s, respectively, without any other impurities. In the NPG spectra, the appearance of the characteristic peaks at about 400eV confirms the successful doping of nitrogen atoms in graphene matrix. As observed in Figure S2b-d, in the high-resolution spectra of the samples, the C1s band can be fitted into three peaks. The C1s band of PG is divided into three distinctive regions at 284.5, 285.8, and 288.6 eV, corresponding to C-C/C=C, C-O and O-C=O bonds, respectively (Figure S2b). The C1s bands of the nitrogen doped samples, specifically C-C/C=C and C-O, exhibit the up-shift toward slightly higher biding energy, signifying the formation of C-N bonds during nitrogen doping treatment (see Figure S2(c-f)). [11] The area ratio of (C-C or C=C) to (C-N or C-O) is apparently decreased by increasing the amount of OPDA, indicating the creation of C-N bands and therefore decreasing the content of C-C or C=C bands after nitrogen doping. Moreover, the area of C-N bands is increased by increasing the concentration of OPDA and maximized at the ratio of 1:5, which further confirms the optimum ratio of the nitrogen doped porous graphene. The high resolution N1s spectra of the nitrogen doped porous graphene can be resolved into four components (Figure S3). Generally, the pronounced peaks centred at ~398.7, 399.5, 401.1, and 403.8 eV can be assigned to pyridinic, pyrrolic, graphitic, and oxidized type of nitrogen atoms, respectively.[12] Nitrogen contents of the NPG 1-0.5, NPG 1-1, NPG 1-10, and NPG 1-5 are calculated to be about 4.1, 6.3, 7.7, and 8.4, respectively (Table 4, main paper). Apparently, the nitrogen content increases by increasing the ratio of OPDA to porous graphene and the optimized ratio (NPG 1-5) shows the highest content of nitrogen atoms.

The nitrogen adsorption-desorption was also carried out to evaluate the porous structure of electrocatalysts. The adsorption-desorption isotherms, the corresponding pore size distribution of non-doped porous graphene (PG) and the optimised nitrogen doped porous graphene (NPG 1-5) are presented in Figure S4. According to the IUPAC classification, the isotherms show a typical curve (type IV) along with a hysteresis loop beginning at the relative pressure of 0.45, signifying the presence of slit shaped mesopores on the graphene sheets.[13] The isotherms and corresponding pore size distribution curves of PG and NPG 1-5 are analogous, indicating the existence of mesoporous structure after nitrogen doping. However, the determined BET specific surface area of NPG 1-5 slightly decrease, which can be attributed to the decrease of the external surface area emanating from nitrogen doping. The BET surface area ($m^2 g^{-1}$), pore volume ($cm^3 g^{-1}$) and mean pore size (nm) for PG sample is 721.3, 2.3 and 12.6, respectively. Also, The BET surface area ($m^2 g^{-1}$), pore volume ($cm^3 g^{-1}$) and mean pore size (nm) for NPG 1-5 sample is 665.2, 1.8 and 13.7, respectively. In addition to BET surface area, the pore volume and pore size of the PG and NPG 1-5 remains approximately unchanged, indicating that nitrogen doping does not principally deteriorate the mesoporous structure of porous graphene, which is in good agreement with TEM images and Raman spectra. The results show that apart from the important role of high surface area and porosity for ORR, the presence of nitrogen along with porous structures not only maintains the mesoporous structure, but also facilitates the reduction of oxygen.[14]

It has been theoretically and experimentally ascertained that all of the N species would provide active sites for ORR.[15] In particular, pyridinic and graphitic nitrogen atoms play a pivotal role in ORR due to donation of one π-electron to the aromatic ring, which leads to facilitation of electron transfer from the carbon electronic bands to the anti-bonding orbitals of O_2. [16-18] As seen within the Supporting information and manuscript Table 4, NPG 1-5 has the highest content of pyridinic and graphitic nitrogen compared to the other samples. However, the content of graphitic nitrogen remained almost unchanged, indicating that the nitrogen doping of porous graphene via OPDA created higher pyridinic nitrogen as the favourable active sites for ORR. Hence, the as prepared nitrogen doped porous graphene in this work, with high content of pyridinic and graphitic, can be applied as a high performance electrocatalyst in ORR (For comparison see Supporting information, Table 1). The XPS spectra along with Raman and XRD have shown that porous graphene was successfully nitrogen doped.

Figure S1. SEM images and mapping analysis of nanoporous graphene (PG) the scale bars in all photos is 2 µm.

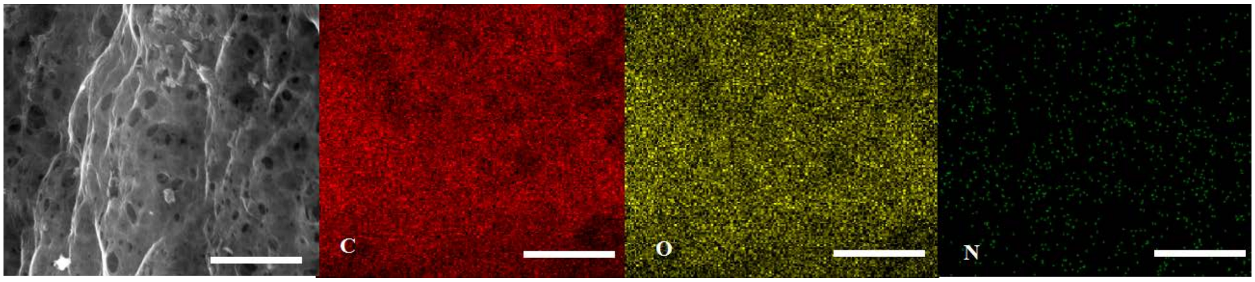

Figure S2. XPS spectra of (a) wide survey of electrocatalysts and C1s high resolution spectra (b) PG, (c) NPG 1-0.5, (d) NPG 1-1, (e)NPG 1-10, and (f) NPG 1-5.

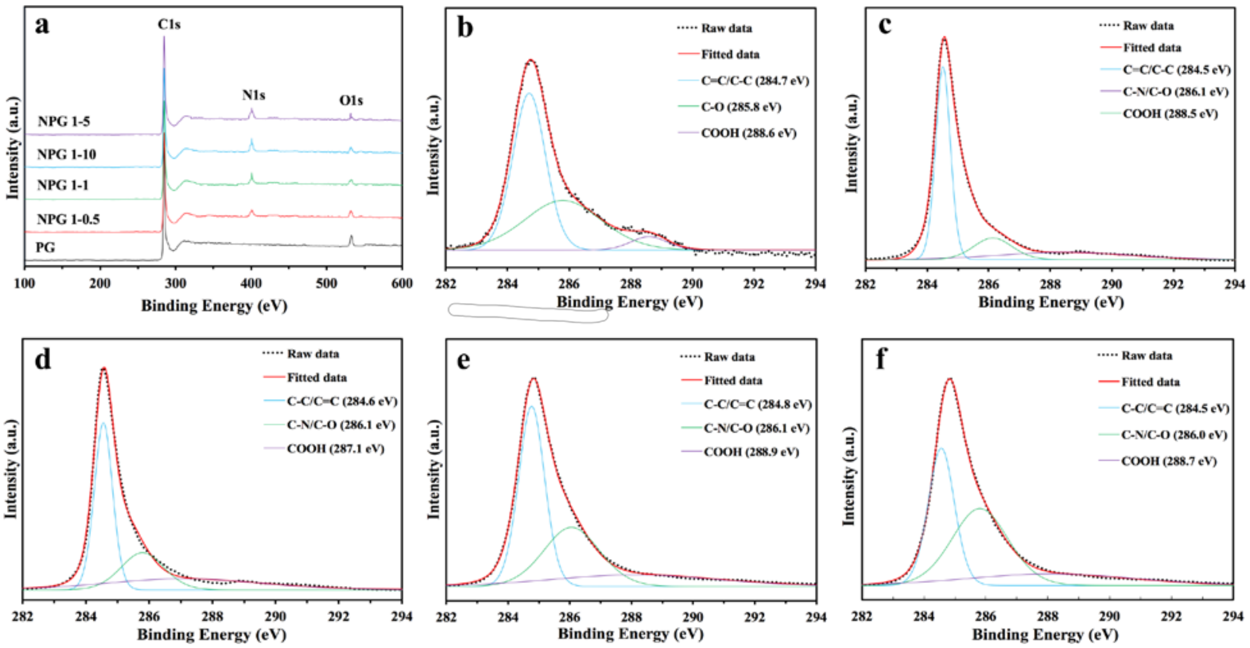

Figure S3. N1s high resolution spectra of (a) NPG 1-0.5, (b) NPG 1-1, (c) NPG 1-10, and (d) NPG 1-5.

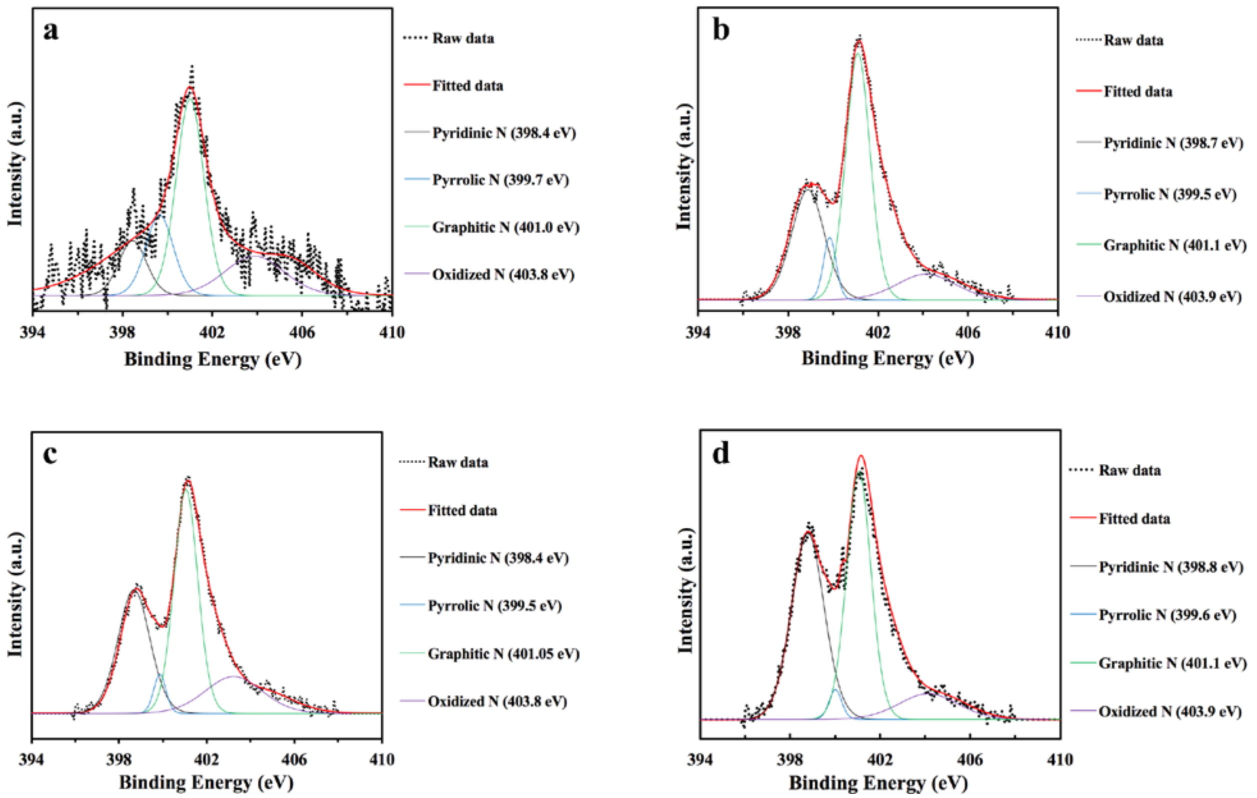

Figure S4. (a) BET isotherms and (b) BJH plots (adsorption branch) of nanoporous and nitrogen doped nanoporous graphene.

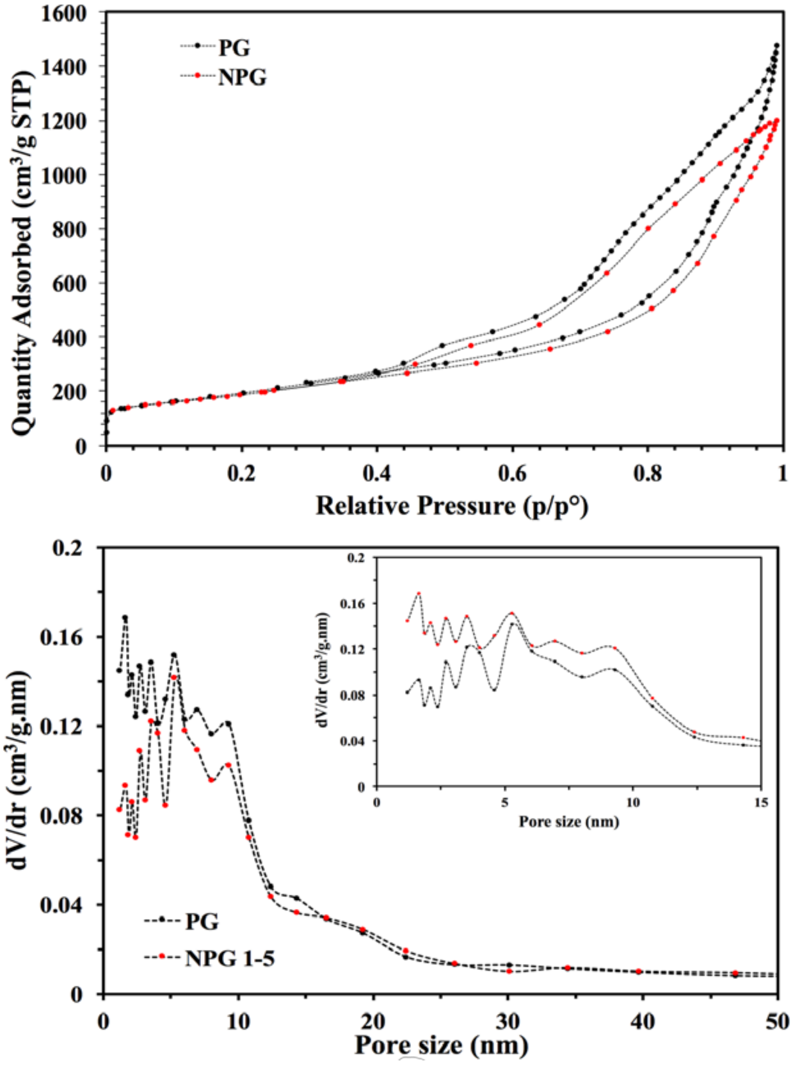

Figure S5. Cyclic voltammetry of (a) NPG 1-0.5, (b) NPG 1-1, (c) NPG 1-10, (d) NPG 1-5, (e) PG, and (f) Pt 20% in KOH 0.1 M 25°C (scan rate: 50 mV sec^{-1}).

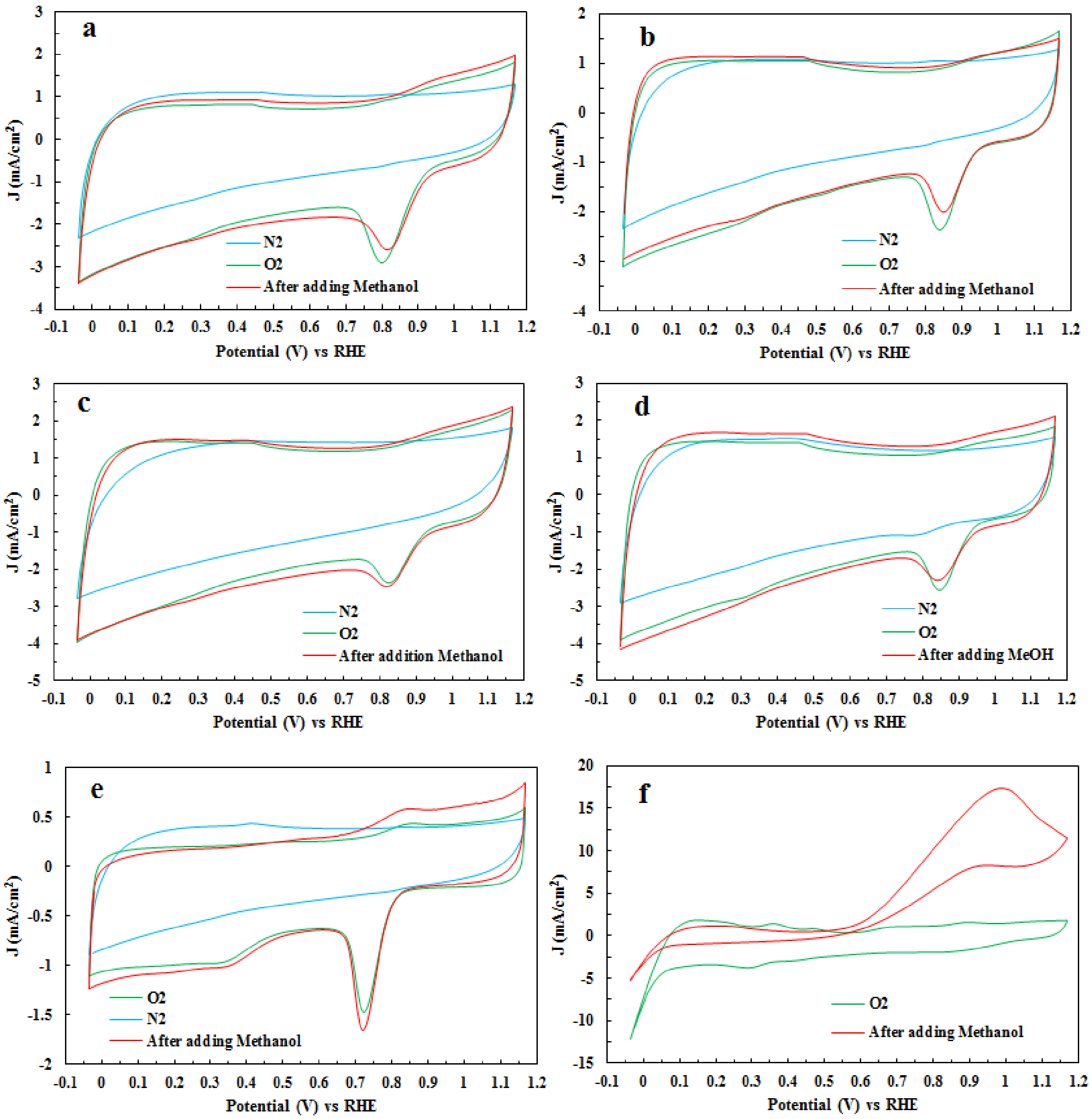

Figure S6. Linear sweep voltammetry at different rotation rate (a) NPG 1-0.5, (b) NPG 1-1, (c) NPG 1-10, (d) NPG 1-5, (e) PG, and (f) Pt/C 20% in KOH 0.1 M, 25^{o}C (scan rete 5 mV/sec).

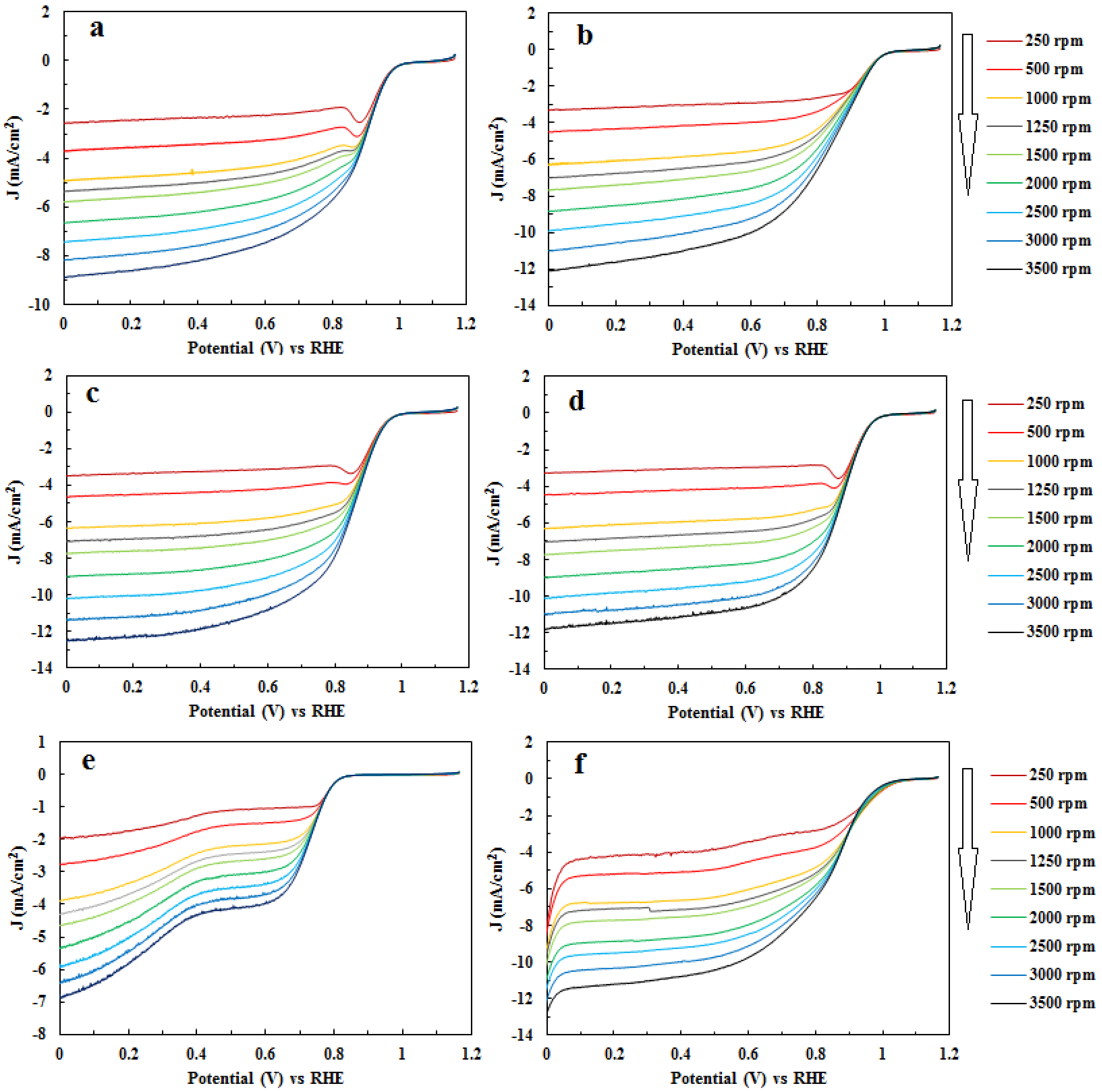

Figure S7. Koutecky-Levich plots of J-1 versus ω^{-1} at various potentials (RHE) from RDE measurements (a) NPG 1-0.5, (b) NPG 1-1. (c) NPG 1-5, (d) NPG 1-10, (e) PG, and (f) Pt/C 20%.

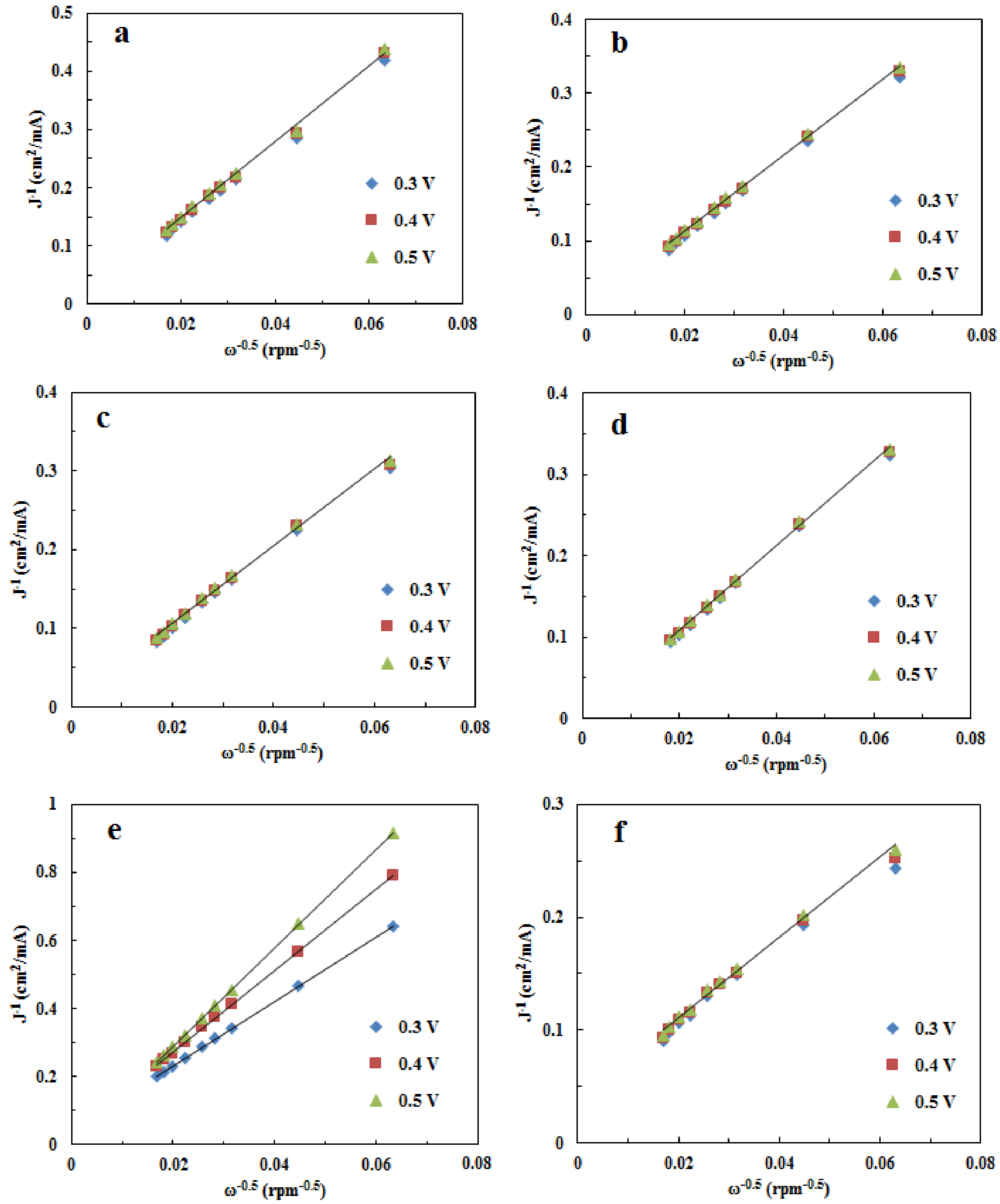

Figure S8. Chronoamperometry at 1.0 V (RHE) and 1500 rpm in 0.1 M KOH O_2 saturated (a) NPG 1-0.5. (b) NPG 1-1. (c) NPG 1-5, (d) NPG 1-10, (e) PG, and (f) Pt/C 20%.

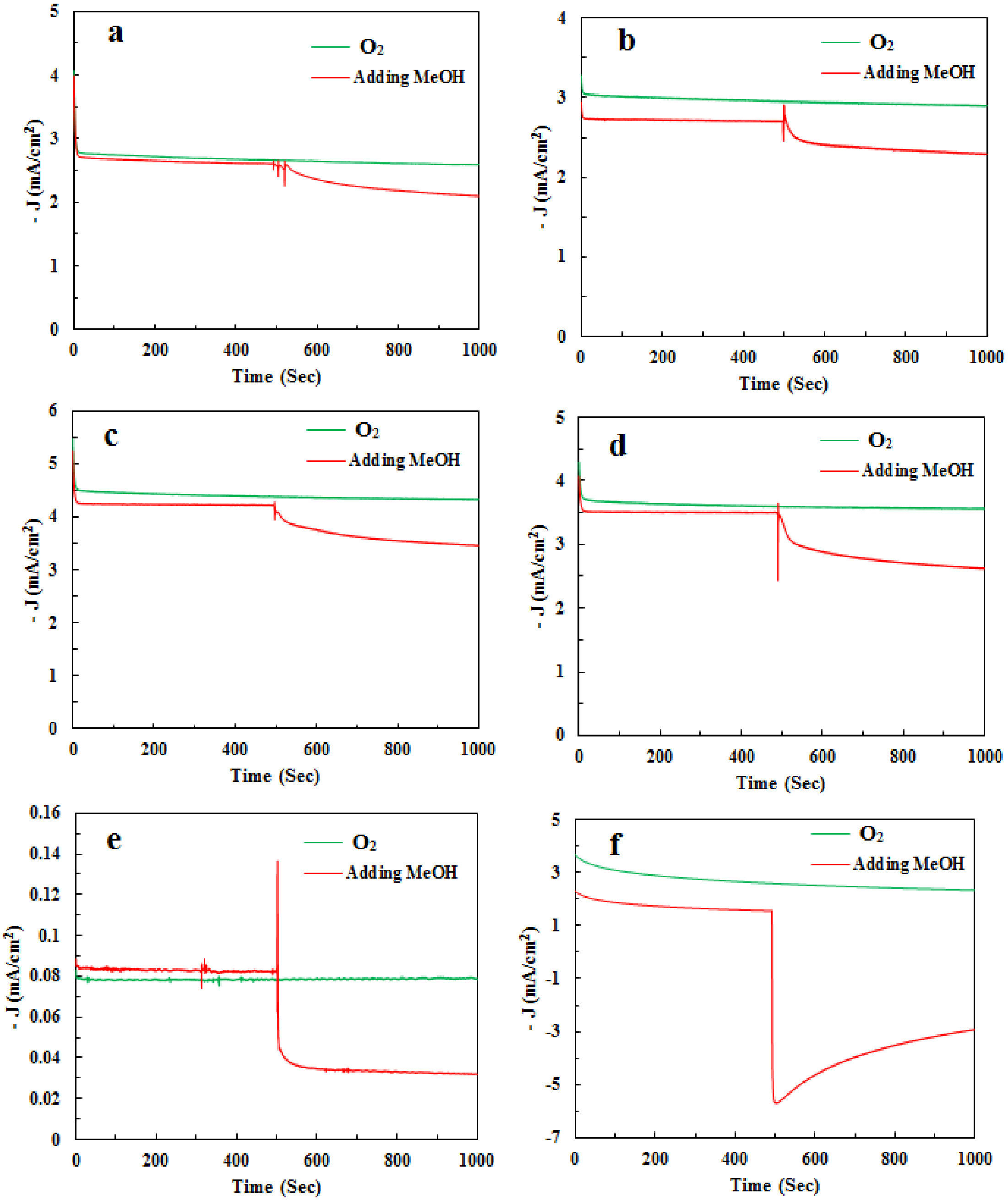

Figure S9. Chronoamperometry at 1.0 V (RHE) and 1500 rpm and (b) Normalized chronoamerometry for the electrocatalysts and comparison of cyclic voltammetry for the PG, the variants and Pt/C 20%. Solution composition: 0.1 M KOH (O_2 saturated).

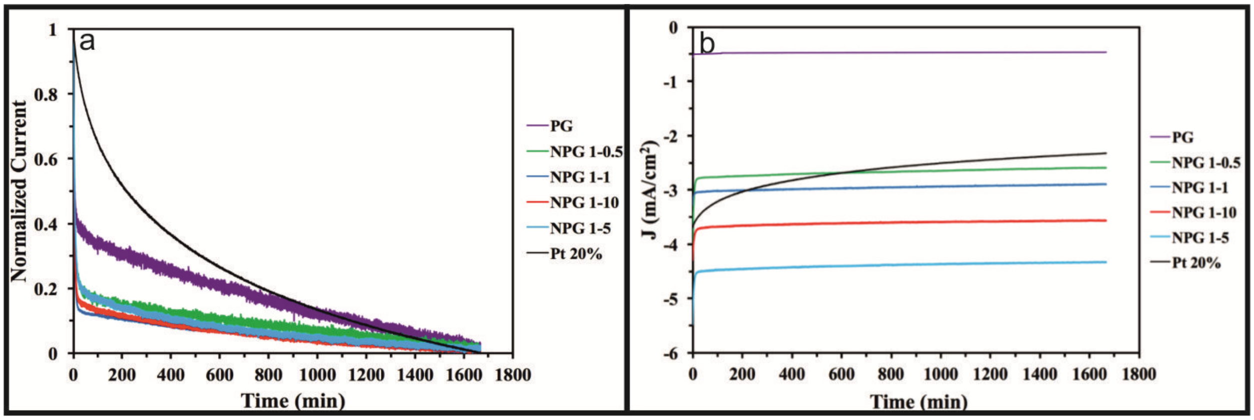

Figure S10. Impedance spectroscopy of (a) NPG 1-0.5, (b) NPG 1-1. (c) NPG 1-10, (d) NPG 1-5, (e) PG, and (f) Pt/C 20% at various applied potentials (RHE) at 1500 rpm in 0.1 M KOH O_2 saturated.

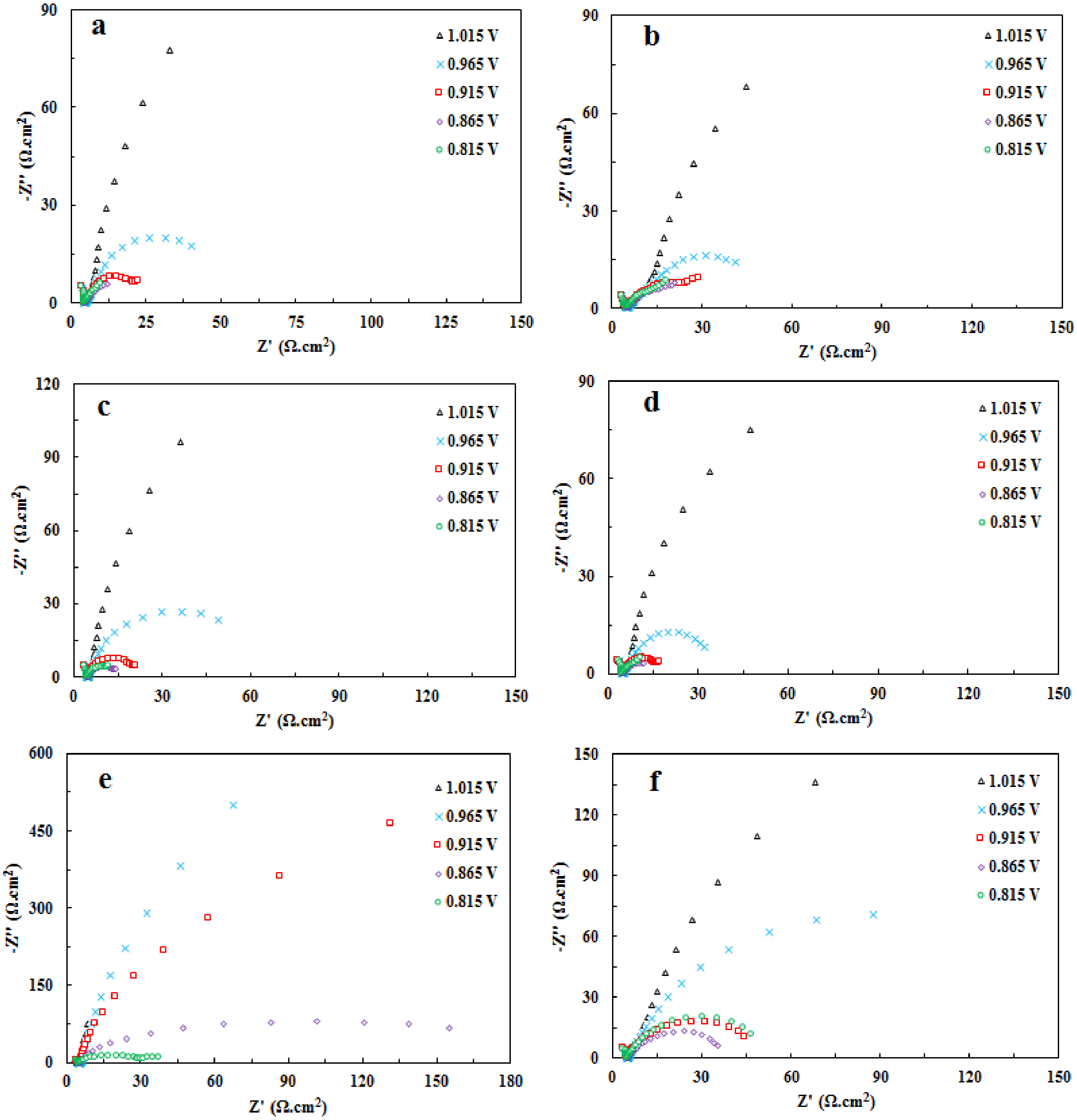

Figure S11. Comparison of impedance spectroscopy at +0.87V (RHE).

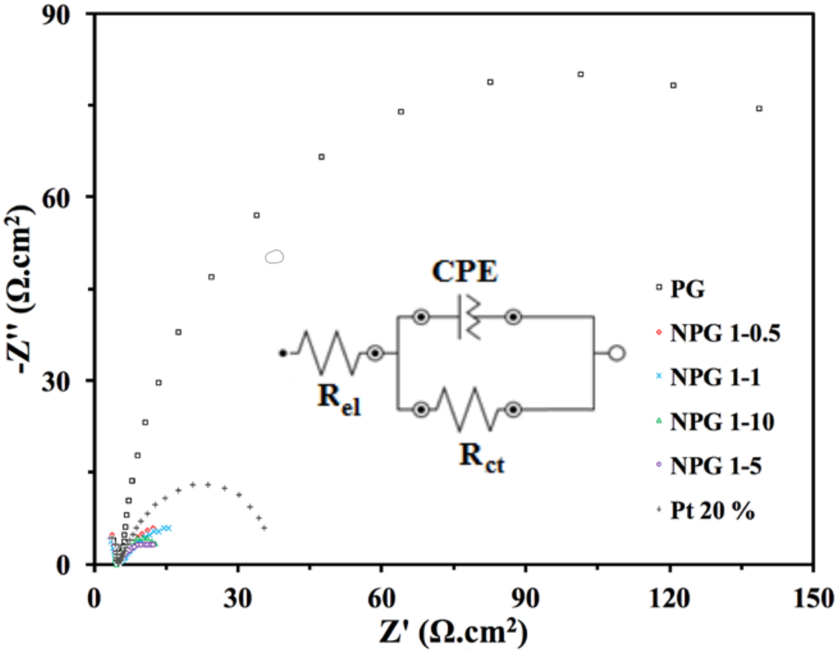

References

11. C. H. Choi, M. W. Chung, H. C. Kwon, J. H. Chung and S. I. Woo, *Appl. Catal., B*, 2014, 144, 760-766.
12. F. Zheng, Y. Yang and Q. Chen, *Nat. Commun.*, 2014, 5.
13. S. Brunauer, L. S. Deming, W. E. Deming and E. Teller, *J. Am. Chem. Soc.*, 1940, 62, 1723-1732.
14. W. J. Jiang, J. S. Hu, X. Zhang, Y. Jiang, B. B. Yu, Z. D. Wei and L. J. Wan, *J. Mater. Chem. A* 2014, 2, 10154-10160.
15. H. Wang, T. Maiyalagan and X. Wang, *ACS Catal.*, 2012, 2, 781-794.
16. Y. Huang, P. Wu, P. Wang, W. Wang, D. Yuan and J. Yao, *J. Mater. Chem. A*, 2014, 2, 19765-19770.
17. T. Xing, Y. Zheng, L. H. Li, B. C. C. Cowie, D. Gunzelmann, S. Z. Qiao, S. Huang and Y. Chen, *ACS Nano*, 2014, 8, 6856-6862.
18. J. Xu, G. Dong, C. Jin, M. Huang and L. Guan, *ChemSusChem*, 2013, 6, 493-499.